



Article

A Model of the Degradation Process of Stone Architecture Under the Influence of Climatic Conditions Described by an Exponential Function [†]

Marek Skłodowski 10 and Alicja Bobrowska 2,*

- Institute of Fundamental Technological Research, Polish Academy of Sciences, Pawińskiego 5B, 02-106 Warsaw, Poland; msklod@ippt.pan.pl
- Faculty of Geology, Department of Geomechanics, University of Warsaw, Żwirki i Wigury 93, 02-089 Warsaw, Poland
- * Correspondence: a.bobrowska@uw.edu.pl
- [†] Some preliminary results of this study are presented in preprint format as: Skłodowski, M.; Bobrowska, A. A generalized exponential function model of the integrity loss of stones subjected to laboratory weathering cycles. 2020. https://doi.org/10.31224/osf.io/dtyac.

Abstract

In assessing the strength properties of stone materials, especially in historic structures, ultrasonic measurements are widely used as a non-destructive testing (NDT) method. Actual stone degradation in situ is estimated based on various laboratory tests which allow researchers to correlate the number of artificial ageing cycles of stone specimens with ultrasonic wave velocity measured on these specimens. This paper presents the results obtained for granite, marble, limestone, travertine and sandstone which underwent various cyclic ageing tests including freezing and thawing, high temperature and salt crystallization. Analysis of the obtained results shows that, independent of the stone type tested and independent of the ageing test applied, a rate of change in the stone elastic properties is described by an ordinary differential equation whose solution is an exponential law analogue to the Newton's law of cooling. The degradation function model can be used for further research on expected residual strength and dynamics of the heritage materials degradation processes.

Keywords: rock engineering; stone deterioration; decay function model; monuments; ultrasonic measurements; cyclic ageing



Academic Editors: Yang Zou, Zongze Li and Marion Fourmeau

Received: 27 October 2025 Revised: 20 November 2025 Accepted: 24 November 2025 Published: 26 November 2025

Citation: Skłodowski, M.; Bobrowska, A. A Model of the Degradation Process of Stone Architecture Under the Influence of Climatic Conditions Described by an Exponential Function. *Appl. Sci.* **2025**, 15, 12552. https://doi.org/ 10.3390/app152312552

Copyright: © 2025 by the authors. Licensee MDPI, Basel, Switzerland. This article is an open access article distributed under the terms and conditions of the Creative Commons Attribution (CC BY) license (https://creativecommons.org/licenses/by/4.0/).

1. Introduction

Contemporary rock engineering focuses on understanding the geotechnical properties of rocks used as a construction material in the structural and decorative elements of stone objects, particularly in the context of their susceptibility to the deterioration processes caused by atmospheric factors. This issue becomes especially important for historic stone monuments, which are often severely degraded and require effective conservation measures to ensure their durability. In rock engineering, geomechanical investigations play a key role in diagnosing the susceptibility of natural rock materials to geo-environmental hazards and loss of strength, and, consequently, the process of destruction of the stone structure.

Stone material ageing is a process of natural degradation of mechanical and decorative properties of stones due to long lasting environmental processes [1]. In geology, these processes are related to the weathering of stone material [2].

The susceptibility of a stone to weathering depends on its morphological and physical-mechanical properties, environmental conditions and exposure time. The ageing process dynamics can hardly be observed in natural conditions because of their slowness. An important role of engineering geology is the assessment of actual and future dynamics of stone material degradation and its susceptibility to environmental loadings. The deterioration processes adversely change structural and esthetic properties of stone material. This problem is economically important also in Poland, which has a long tradition of using stone structural and decorative elements in heritage buildings. Nowadays, civil engineering and the esthetic use of stones also pursue the research on the dynamics and modelling of deterioration processes.

Engineering geology developed geomechanical research methods for non-invasive diagnostics of stone susceptibility to environmental risks. These methods can be studied in laboratories [3,4] and advantageously forecast stone integrity based on geomechanical tests of accelerated ageing. Measured values of, e.g., ultrasonic wave velocity, rebound hardness, strength, etc., can be plotted against the number of cycles of the ageing, and the observed trend extrapolated to predict the further decrease in stone elastic properties. There are also papers presenting a deeper insight in stone deterioration mechanisms; however, they publish fresh and degraded stone material properties after a one-time period or one number of cycles without intermediate stages, which does not inform about the dynamics of deterioration processes [5–7], or valuable works showing deterioration trends in graphical or mathematical form with insufficient information, however, about measurement data to allow the reader to analyze the results by himself [8].

Comparing the impact of various deterioration processes, it is possible to determine the dominating and less important environmental factors for various building materials. To this purpose, more interesting than simple mathematical extrapolation of the test results is having a physical model of the stone deterioration process, and of the degradation of its properties. The interesting idea was presented by Mutlutürk et al. in 2004 [9] of adopting a well-known radioactive decay function to this purpose. The same decay function was used to describe a decrease in the compressive strength of natural hydraulic lime mortar due to varying leaching time [10].

In 2005, the Mutlutürk model was considered to describe stone durability under various ageing processes within EC Project MCDUR (McDUR—Effects of the weathering on stone materials: assessment of their mechanical durability—(Contract G6RD-CT2000-00266)//(EC FP5, GROWTH, 2002–2005)), and a generalized version of the decay function called fatigue law there, with non-zero asymptotic stone integrity level (residual integrity), was proposed by Exadaktylos and analyzed by the Project Partners. According to the authors' best knowledge, it has not been published except in MCDUR Final Report [11].

In this paper, the resilience of stones from Mediterranean Basin and Poland is analyzed to determine the deterioration processes and the influence of moderate and Mediterranean climates' environmental conditions on these processes. The process is modelled by the exponential law proposed in MCDUR, being the general exponential decay function analogues to the Newton's law of cooling.

The analyzed rock materials are commonly used raw construction materials, found in both small- and large-scale architecture as structural and decorative stone elements.

Some preliminary results of this study are presented in preprint format as https://doi.org/10.31224/osf.io/dtyac [12]. This paper presents the same experimental results, but specimens and testing are now described in more details, and the discussion and conclusions section is refined to ensure greater clarity and understandability of the paper's main idea.

2. Tested Stone Materials

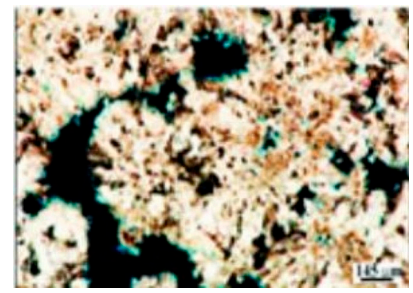
The tested stone materials from the Mediterranean Basin are represented by Gioia Marble (MG), Italy, and travertine from Pamukkale (PA), Turkey. These stones have been used as structural and decorative materials both in ancient times and nowadays. The stones from Poland, represented by sandstone from Szydłowiec (SZ), granite from Strzegom (ST) and limestone from Raciszyn (RA), known under the technical name "Polish travertine", are the stones used in construction today for internal and outside cladding. Travertine, marble, sandstone and limestone were fresh from a quarry, while granite was displaced from XIX c. grave tombs during conservation works [13]. The petrographic characteristics of the analyzed rock materials, based on thin sections analysis, are presented in Table 1.

Table 1. General petrographic characteristics of tested stone materials.

Genetic Type/Quarry

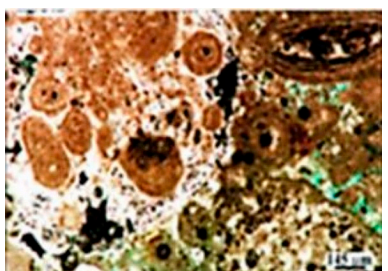
Sedimentary rocks

Travertine/Pamukkale (Turkey) (PA) Crystalline limestone (sparry) **, from the Late Pleistocene age



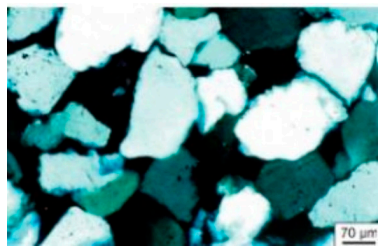
The rock skeleton consists of a polycrystalline sparry structure formed by interlocking calcite crystals of varying sizes ranging from 0.10 to 0.50 mm, predominantly exhibiting an elongated, coarsely lamellar morphology. The calcite crystals are arranged in characteristic forms within the rock, including speleothem, rosette, and conical shapes. Within these formations, alongside the predominantly polycrystalline sparry structure, small carbonate micritic accumulations are present.

Limestone/Raciszyn (Poland) (RA)
Pakston biolithite **/calcareous pakston with ooids, from the
Jurassic period



The rock exhibits a biomorphic structure, macro-porous, with a matrix composed of organic fragments and pseudo-oolites cemented by fine-grained calcite. The rock skeleton consists of numerous, randomly oriented, interlocking granular components. Oval ooids, ranging in size from 0.10 to over 1.5 mm, dominate the composition. The ooid aggregates are typically coarse, composed of calcitic micrite, and often display a visible concentric structure. In some cases, the entire interior of the ooid is recrystallized (sparry), and in certain instances, it is secondarily cemented by spar. Bioclasts are present in smaller quantities.

Sandstone/Szydłowiec (Poland) (SZ) Sublithic arenite *, a medium-grained sandstone with a siliceous cement, from the Lower Jurassic period



The fine-grained structure is well-sorted, with a characteristic quartz cement in the form of regenerating rims, along with locally occurring siliceous-clayey cement in the form of small clusters. The composition is nearly monomineralic, consisting of weakly rounded quartz grains (97%), predominantly isometric in shape, and ranging in size from 0.08 to 0.15 mm. Additionally, there is a presence of small amounts of polycrystalline quartz grains and fragments of quartzose rocks. Zircon and yellow tourmaline grains occur sporadically.

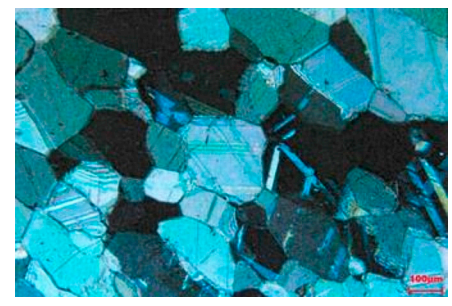
Igneous rocks Metamorphic rocks

Granite/Strzegom (*Poland*) (*ST*) Granitoid *** Medium-grained granite with a massive, chaotic structure, from the Variscan age.



The biotite granodiorite is light grey, equigranular and slightly foliated, the foliation locally being accentuated by the presence of lens-shaped quartz aggregates. It is composed of plagioclase (36–48% modally), K-feldspar (20–25%), quartz (23–35%) and biotite (3–6%), with accessory zircon, apatite, allanite, monazite, xenotime and opaque minerals. The plagioclase forms subhedral to euhedral prisms. K-feldspar and quartz form inclusions. Alkali feldspar forms mainly anhedral crystals. Biotite inclusions are present, and Quartz occurs as anhedral.

Marble/Carrara (*Italy*) (MG) Marble, fine-grained, with a chaotic structure, from the Lower Jurassic period.



The texture is of the polygonal grain-like type. The calcite crystals have dimensions between 0.05 mm (rare) and 0.3 mm, the average size is about 0.2 mm; the outlines ale clear. There are numerous geminated calcite crystals. Composition: calcite for over 95%, accessory dolomite.

^{*} Rock classification according to Pettijohn, Potter and Siever (1972 [14]); ** Rock classification according to Dunham (1962) [15]. *** Classification according to IUGS/According to Standard EN 12407 "Natural stone test methods—Petrographic examination" 2007 [16].

Appl. Sci. 2025, 15, 12552 4 of 13

Laboratory tests of the physical and mechanical properties (bulk density, total porosity, water absorption, uniaxial compressive strength) and longitudinal ultrasonic wave propagation analysis of the examined rocks were carried out on standard cylindrical samples with dimensions of 50 mm diameter and 51 \pm 4 mm height for rocks from Poland (sandstone from Szydłowiec (SZ), granite from Strzegom (ST), limestone from Raciszyn (RA)) and Turkey (travertine from Pamukkale (PA)). The marble samples of Gioia (MG) from Italy were rectangular prisms measuring 100 mm \times 50 mm, in accordance with the guidelines of the McDUR project. The summary of the physical and mechanical properties of the tested stone materials is presented in Table 2.

Table 2. Physical and mechanical properties of tested stone materials.

Stone Material	Parameter Average Value	Real Density ρ [kg/m³]	Bulk Density $ ho_{ m b}$ [kg/m 3]	Total Porosity n [%]	Water Absorption [%]	Longitudinal Wave Velocity Vp [m/s]	Uniaxial Compressive Strength Rc [MPa]
MG		2716	2708	0.76	0.28	1900	109
PA		2010	1790	23.70	5.75	3950	17
SZ		2670	1940	27.38	9.60	2980	46
ST		2670	2590	2.88	0.52	2680	121
RA		2680	2450	8.72	2.72	5225	44

The selected stones represent sedimentary, metamorphic and igneous stones and cover a broad range of these properties. For example, uniaxial compressive strength varies from 17 MPa to 109 MPa for Mediterranean stones, and from 43 MPa to 121 MPa for stones from Poland. Similar observations can be achieved in the case of other stone properties. These allowed us to analyze dynamics of degradation processes for a relatively large variety of stone materials and present conclusions regarding the possibility of efficient modelling of stone integrity loss being an interesting and practically important geomechanical problem.

3. Laboratory Methods of Deterioration Testing

The susceptibility of the analyzed/selected rocks to the deterioration processes was determined on the basis of ultrasonic tests of samples seasoned in various environmental conditions. Rock samples with known initial parameters were seasoned under cyclic freezing (A) freezing and thawing (F/T) conditions of marble, granite, limestone and travertine in the following temperature range: $-25\,^{\circ}\text{C} \div 20\,^{\circ}\text{C}$ (248 K $\div 293\,\text{K}$), in accordance with the standard PN-EN 12371: 2010 [17]. The effect of insolation, i.e., artificial sunlight on sandstone, granite, limestone and travertine at a temperature of 40 $^{\circ}\text{C}$ (313 K), was tested in order to simulate the action of sunlight in the Mediterranean and temperate climate zone, in accordance with the original procedure developed by the second author (AB) [18]. Seasoning in a salt solution (crystallization of limestone and travertine salts) was performed, in accordance with the recommendations of the standard PN-EN 12370:2001 [19]. The marking consisted in a cyclical (15 times) placing of rock samples dried at 105 $^{\circ}\text{C}$ (378 K) in a 14% solution of decahydrate solution of sodium sulfate.

Non-destructive testing (NDT) of stones has the main advantage of using the same specimens throughout the whole research programmes—from an origin stone state and after each cycle of laboratory accelerated ageing. Thus, measurement results in each cycle are performed on the same material and not influenced by possible differences between various specimens. Ultrasonic measurements are among the most often used NDT methods because of their reliability, ease of use and direct relation of the sound propagation velocity V to modulus of elasticity E of the material $(V^2 \sim E)$. Assuming the Continuum Damage Mechanics damage model of the material [20] with scalar damage parameter

 $DN = 1 - E_N/E_0$ [21,22], the material integrity $I_N = 1 - D_N$ after N deterioration cycles is equal to E_N/E_0 and hence.

$$I_{N} = \frac{E_{N}}{E_{0}} = \left(\frac{V_{N}}{V_{0}}\right)^{2} \tag{1}$$

where E_N , V_N are the elasticity modulus and wave propagation velocity after N cycles and E_0 , V_0 represent the elasticity modulus and the ultrasonic wave velocity recorded at the beginning of the ageing experiments.

Non-destructive ultrasonic measurements of V_P and V_R velocities were made to test the weathering behaviour of five stones with known physical and mechanical properties. Longitudinal waves V_P were measured in transition mode on granite, sandstone, travertine and limestone along the height of the cylindrical specimens having 50 mm in diameter and the slenderness equal to 1. Ultrasonic V_P probes had frequency of 1 MHz and 0.5 MHz.

Rayleigh surface wave V_R [23] was measured on side walls of the prismatic marble specimen using edge probes emitting 2 MHz ultrasonic wave. The time of flight of ultrasonic waves was recorded and sound velocity calculated for known travel distance. In each measurement case, several recordings were performed and the average ultrasound velocity values were calculated. The ultrasound velocity values before laboratory weathering are presented in Table 2.

The following geomechanical accelerated ageing tests were applied:

- (A) Freezing and thawing (F/T) of the marble, granite, limestone and travertine in the temperature range (-25 °C \div 20 °C) (248 K \div 293 K) according to Standard (PN-EN 12371: 2010) [17];
- (B) Artificial insolation of the sandstone, granite, limestone and travertine, at 40 °C (313 K) to simulate sun operation at Mediterranean and moderate climatic zones according to the originally developed procedure by the second author (AB) [18];
- (C) Salt crystallization for the limestone and travertine according to Standard (PN-EN 12370: 2001) [19].

4. Theoretical Model of Stone Deterioration

Mathematical modelling of stone deterioration processes can be performed using thermo-physical models [24], requiring many material parameters and extensive computer calculation time. Opposite to rigorous theoretical analysis, it is reasonable to look for phenomenological description of stone deterioration. The main reason is operational suitability to geotechnical analysis, ease of use and neglecting the local variations in material parameters influencing the complicated thermo-physical-mechanical modelling results. A good phenomenological model can describe material deterioration with statistically acceptable accuracy at relatively low experimental and calculation costs. However, it should not be simply a function approximating experimental data. For a model, it is required to describe the law governing observed deterioration phenomena, otherwise deterioration processes of various stones under various environmental loadings could not be compared among each other.

An interesting and simple phenomenological model was suggested by Mutlutürk and co-author [9] and verified for 10 various stone types (limestones, marbles, travertines and diabase) using Shore hardness SH index (scleroscope method) as a measure of stone integrity. The authors observed that decay law known, e.g., for describing the decay of radioactive elements can describe their experimental observations well. In this case, the rate of loss of a stone integrity I is proportional to its integrity at the beginning of the each ageing cycle N.

$$-\frac{\mathrm{dI}}{\mathrm{dN}} = \lambda \mathrm{I} \tag{2}$$

where -dI/dN is a disintegration rate (integrity loss rate) and λ a positive constant number called decay constant. Integrity I equals to 1 for a non-deteriorated material and equals to zero in the case of complete degradation.

The solution of this differential equation is

$$I_{N} = e^{-\lambda N} \tag{3}$$

where λ is a decay constant, which shows that stone integration I_N after N ageing cycles diminishes exponentially with the number of cycles. The law assumes that a stone completely deteriorates and loses its full integrity, which is not always the case and depends on stone properties and environmental degradation factors.

The mathematical model of the generalized deterioration law [11] is based on experimental observations that, in some cases, the final residual integrity is not zero and a continuation of the stone ageing process does not result in its further deterioration. Such a generalized model is analogous to the Newton's law of cooling and is expressed as

$$-\frac{\mathrm{dI}}{\mathrm{dN}} = \lambda(\mathrm{I} - \mathrm{A})\tag{4}$$

which means that, in general, the disintegration rate -dI/dN is proportional to the difference between the actual integrity I and its asymptotic value $A \ge 0$ which is the residual integrity.

The analogy is in mathematical form only as environmental stresses are the real driving forces of the degradation processes, and possible mechanisms governing a relation between environmental stresses and the disintegration rate -dI/dN are not considered in the paper.

Obviously, when there is no residual integrity and a stone completely deteriorates, then A = 0 and Equation (3) becomes the same as (2). The solution of Equation (4)

$$I_{N} = A + (1 - A)e^{-\lambda N} \tag{5}$$

allows us to describe and compare the degradation of stones with zero and non-zero residual asymptotic integrity A.

In the present research, the integrity model was calculated based on measurements of elastic waves propagation velocity using Equation (5), and experimentally measured stone integrity is calculated as Material Elasticity Index (MEI).

$$MEI = \left(\frac{V_N}{V_0}\right)^2 \tag{6}$$

The wave propagation velocity measurements were performed for longitudinal ultrasonic wave for every tested stone except of Gioia Marble, for which ultrasonic surface Rayleigh wave was used.

5. Results and Discussion

Measured ultrasonic wave velocities before and after the deterioration cycles for the tested stones and various applied degradation tests performed in the laboratory of Institute of Hydrogeology and Engineering Geology of Warsaw University are presented in the below tables. MEI values calculated according to (6) are rounded to four meaningful digits.

The presented figures (at the end of the manuscript) are graphical representations of data shown in Tables 3–5. Altogether, 85 experimental data recorded for five stones were analyzed. The results are presented in Figures 1–10, with continuous lines representing the integrity model function calculated according to Equation (5), and discrete points show

Appl. Sci. 2025, 15, 12552 7 of 13

experimental MEI indices calculated using Equation (6). Asymptotic integrity values A predicted by the model and correlation coefficient Rsq between the data and the model are also given in each figure.

Table 3. (a) Ultrasound velocity (Rayleigh surface wave) in F/T tests for Gioia Marble. (b) Ultrasound velocity in F/T test for Strzegom Granite. (c) Ultrasound velocity in F/T tests for Raciszyn Limestone. (d) Ultrasound velocity in F/T tests for Pamukkale Travertine.

			(a)			
Cycle	0	40	60	80	100	120
V _{N [m/s]}	1900	1600	1500	1450	1300	1500
$(V_{\rm N}/V_0)^2$	1	0.7091	0.6233	0.5824	0.4681	0.6233
Model parameters	Decay constant λ =	0.0251 Residual asymp	totic Integrity A = 0.53	Correlation coefficient	Rsq = 0.9099	
			(b)			
Cycl	le	0	5	10	15	20
V _{N [m}	1/s]	4359	3792	3613	3391	3072
(V _N /V	$(V_0)^2$	1	0.7568	0.6870	0.6052	0.4967
Model parameters		Decay constant $\lambda = 0$	0.087 Residual asympto	otic Integrity A = 0.42 0	Correlation coefficient R	Asq = 0.9765
			(c)			
Cycle	0	5	10	15	20	25
$V_{N[m/s]}$	4942	4895	4895 4816 48		4805	4788
$(V_{\rm N}/V_0)^2$ 1		0.9811	0.9497	0.9576	0.9453	0.9386
Model parameters	Decay constant λ =	0.0814 Residual asymp	totic Integrity A = 0.93	Correlation coefficient	Rsq = 0.9289	
			(d)			
Cycle	0	5	10	15	20	25
$V_{N[m/s]}$	3882	3821	3781	3662	3644	3662
$(V_{\rm N}/V_{\rm 0})^2$	1	0.9688	0.9486	0.8897	0.8811	0.8897
Model parameters	Decay constant λ =	0.0508 Residual asymp	totic Integrity A = 0.83	Correlation coefficient	Rsq = 0.9250	

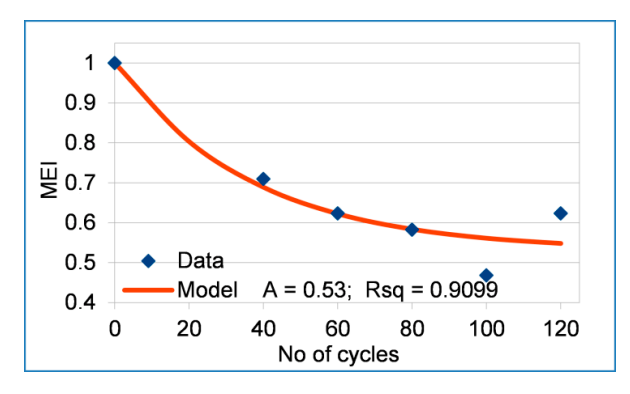


Figure 1. Gioia Marble (IT); Freeze and Thaw test.

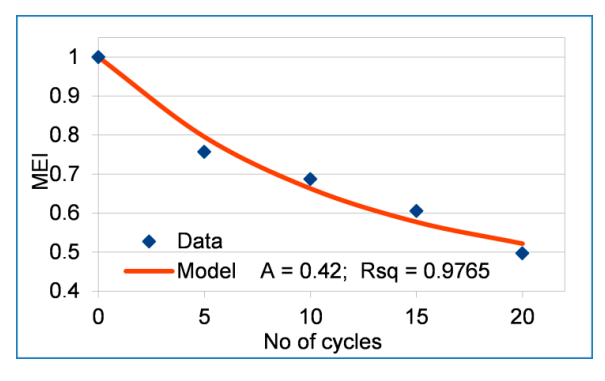


Figure 2. Strzegom Granite (PL); Freeze and Thaw test.

Table 4. (a) Ultrasound velocity in insolation tests for Szydłowiec Sandstone. (b) Ultrasound velocity in insolation tests for Strzegom Granite. (c) Ultrasound velocity in insolation tests for Raciszyn Limestone. (d) Ultrasound velocity in insolation tests for Pamukkale Travertine.

							(a)									
Cycle	0	7	14	21	28	35	42	49				56				
V _{N [m/s]}	3406	3368	3368	3339		3333	3333	3327				3339	9			
$(V_{\rm N}/V_0)^2$	1	0.9778	0.9778	0.9610		0.9576	0.9576	0.9541				0.961	10			
Model parameters	Decay	constant	$\lambda = 0.098$	3 Residı	ıal asym	ptotic Int	egrity A	= 0.96 C	Correlatio	n coeffici	ient Rsq	= 0.930	0			
							(b)									
Cycle	0	7	14	21	28	35	42	49	56	63			70)		
$V_{N[m/s]}$	4132	4063	3987	3755	3583	3488	3258	3222	3250	3190			321	10		
$(V_{\rm N}/V_0)^2$	1	0.9669	0.9310	0.8258	0.7519	0.7126	0.6217	0.6080	0.6187	0.5960			0.60)35		
Model parameters	Decay	constant	$\lambda = 0.017$	8 Residı	ual asym	ptotic Int	egrity A	= 0.39 C	Correlatio	n coeffici	ient Rsq	= 0.956	5			
							(c)									
Cycle	0	7	14	21	28	35	42	49	56	63	70	77	84	91	98	3
$V_{N[m/s]}$	4703	4627	4568	4457	4461	4500	4526	4525	4512	4475	4445	4399	4390	4390	437	71
$(V_{\rm N}/V_0)^2$	1	0.9679	0.9434	0.8981	0.8997	0.9155	0.9261	0.9257	0.9204	0.9054	0.8933	0.8749	0.8713	0.8713	0.86	38
Model parameters	Decay	constant	$\lambda = 0.039$	5 Residı	ıal asym	ptotic Int	egrity A	= 0.8810	Correlatio	n coeffici	ient Rsq	= 0.766	9			
							(d)									
Cycle	0	7	14	21	28	35	42	49	56	63	70	77	84	91	98	105
$V_{N[m/s]}$	4505	4481	4482	4499	4474	4468	4462	4448	4453	4436	4468	4425	4413	4400	4398	4391
$(V_{\rm N}/V_0)^2$	1	0.9894	0.9898	0.9973	0.9863	0.9836	0.9810	0.9749	0.9770	0.9696	0.9864	0.9848	0.9596	0.9539	0.9531	0.9500
Model parameters	Decay	constant	$\lambda = 0.000$	5 Residı	ıal asym	ptotic Int	egrity A	= 0.07 C	Correlatio	n coeffici	ient Rsq	= 0.889	3			

Table 5. (a) Ultrasound velocity in salt crystallization tests for Raciszyn Limestone. (b) Ultrasound velocity in salt crystallization tests for Pamukkale Travertine.

			(a)			
Cycle	0	3	6	9	12	15
V _{N [m/s]}	5021	5009	5004	5001	4999	4997
$(V_{\rm N}/V_0)^2$	1	0.9952	0.9932	0.9920	0.9913	0.9905
Model parameters	Decay constant ?	\ = 0.1906 Residual	asymptotic Integri	ity $\mathbf{A} = 0.99$ Correla	ation coefficient Rs	q = 0.9956
			(b)			
Cycle	0	5	10	15	20	25
V _{N [m/s]}	3627	3607	3599	3598	3594	3589
$(V_{\rm N}/V_0)^2$	1	0.9890	0.9846	0.9841	0.9819	0.9792
Model					ation coefficient Rs	

In Figures 1 and 5, a lack of one measurement data point can be seen. There is no experimental point for 20th F/T cycle of Gioia Marble and for 28th insolation cycle of Szydłowiec Sandstone. In both cases, the measured wave velocities fell outside the 95% error confidence bounds and were rejected.

Appl. Sci. 2025, 15, 12552 9 of 13

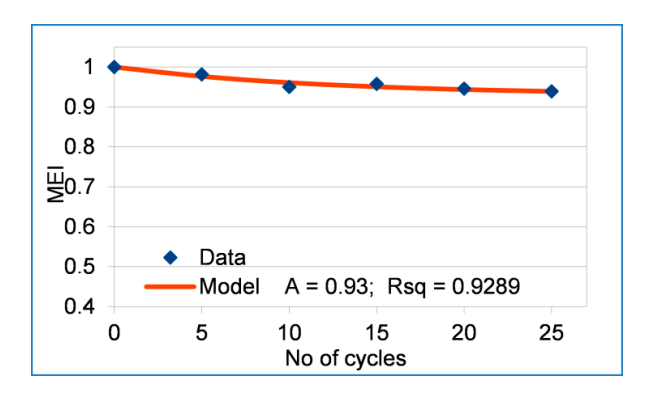


Figure 3. Raciszyn Limestone (PL); Freeze and Thaw test.

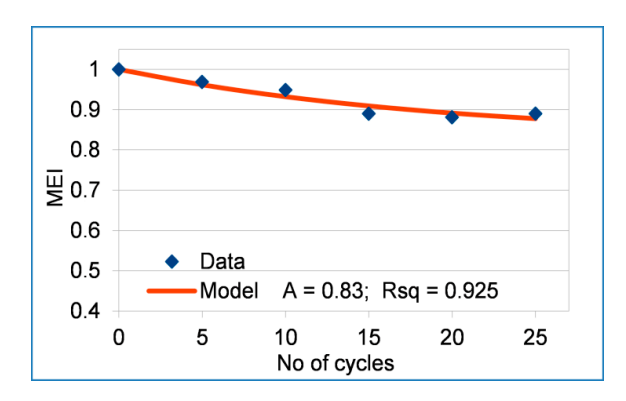


Figure 4. Pamukkale Travertine (TR); Freeze and Thaw test.

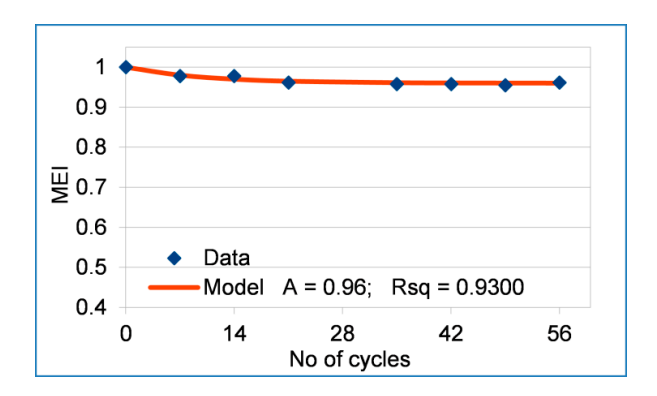


Figure 5. Szydłowiec Sandstone (PL); Insolation test.

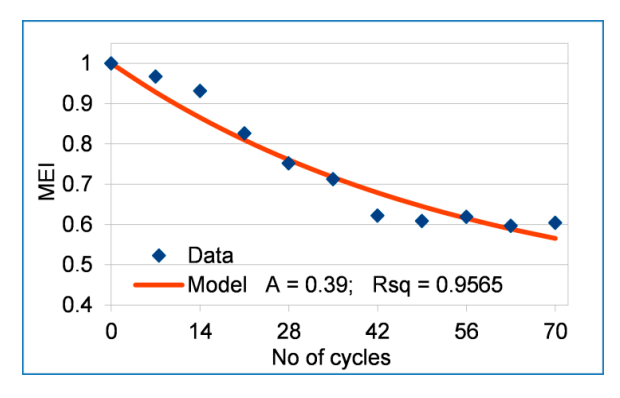


Figure 6. Strzegom Granite (PL); Insolation test.

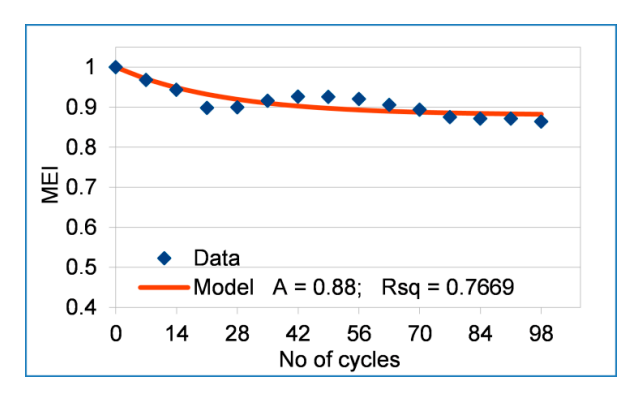


Figure 7. Raciszyn Limestone (PL); Insolation test.

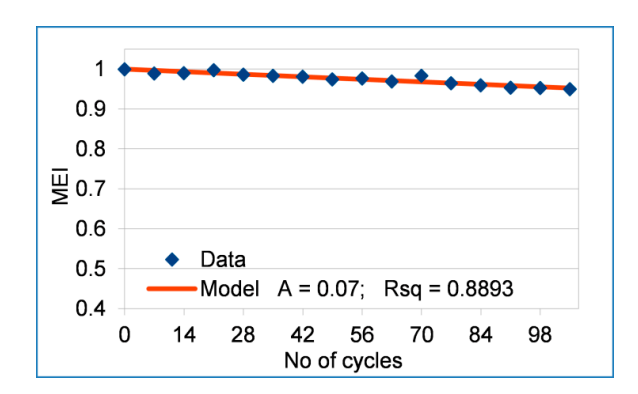


Figure 8. Pamukkale Travertine (TR); Insolation test.

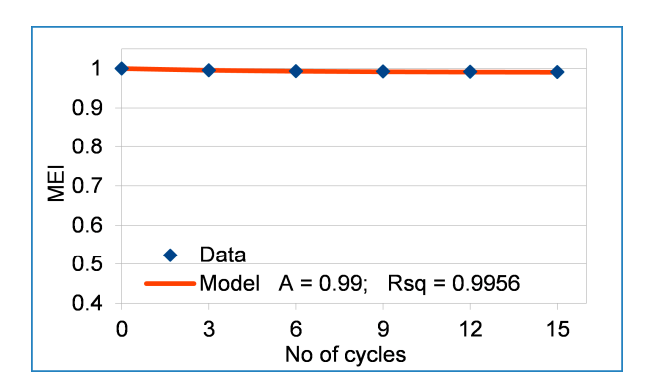


Figure 9. Raciszyn Limestone (PL); Salt crystalisation test.

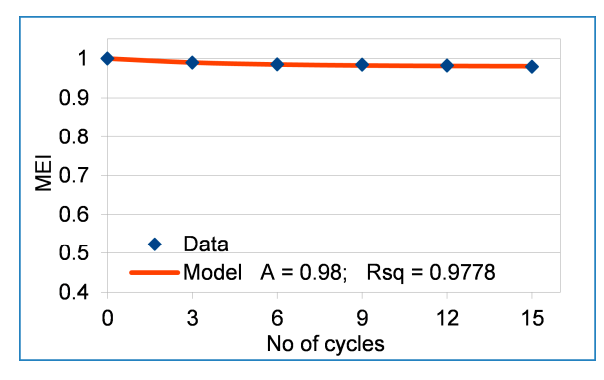


Figure 10. Pamukkale Travertine (TR); Salt crystalisation test.

In nine cases out of ten, the residual integrity A of the tested stones is moderate $(0.39 \div 0.53)$ or high $(0.88 \div 0.99)$. Only Pamukkale Travertine undergoing ageing due to artificial insolation (test type B) shows the residual integrity as low as A = 0.07, but degrades

very slowly—only about 5% of integrity loss after 105 artificial insolation cycles. On the other hand, Pamukkale Travertine sustains in situ tens of thousands of real insolation cycles and still has the integrity greater than zero (monuments still exist). This suggests that developed artificial insolation test is probably much more aggressive than natural environmental loads.

Correlation of MEI with the model is very high in the most cases. The lowest value of Rsq = 0.7669 is for Raciszyn Limestone under insolation ageing.

Calculated model integrity functions allowed us to compare the dynamics of degradation processes under F/T for marble, travertine, granite and limestone. The comparison is presented in Figure 11. Without a well-correlated model, such a comparison would not be possible.

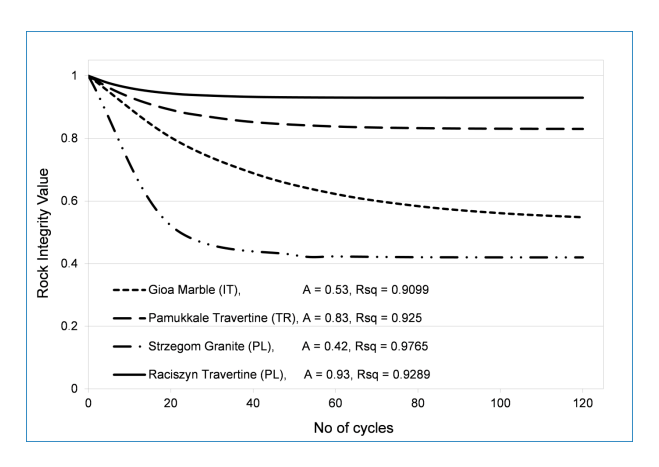


Figure 11. Comparison of generalized decay functions of four stones under freeze and thaw action based on ultrasound R-wave (Marble) and P-wave (Granite, Travertine) velocity measurements.

6. Conclusions and Discussion

Laboratory experiments conducted on the artificial ageing of various stones—including granite, marble, limestone, travertine and sandstone—utilized a combination of freezing and thawing cycles, insolation exposure and salt crystallization tests. These experiments were complemented by the measurement of ultrasonic wave velocities, which provided critical insights into the deterioration of the elastic properties of these stone materials.

The ultrasonic velocities measured during these experiments were instrumental in establishing the Material Elasticity Index (MEI), a quantifiable metric that effectively describes the experimentally observed loss of integrity within the stone material. This index serves as a vital tool for assessing the extent of degradation and provides a basis for understanding the structural viability of stone materials over time.

To further analyze the degradation process, a mathematical model analogous to Newton's law of cooling was developed to describe the degradation of elastic properties in stone. The model demonstrated a strong correlation with the experimental MEIs, suggesting that the relationship between time, environmental stressors, and material degradation follows predictable patterns. The elaborated model of stone degradation can be used for various purposes. Mainly, as a diagnostic tool for evaluation of the advancement of the degradation of building materials existing in heritage structures. The degradation functions derived from the model can be utilized in ongoing research aimed at predicting the residual strength and degradation dynamics of stones in cultural heritage buildings, sculptures and artefacts, and also to compare (using laboratory tests) various materials susceptibility to degradation factors predominant at locations where a new or a replacement material is to

be used. As a case study, the dynamics of degradation among four different types of stone under cyclic freezing and thawing conditions were compared.

The results indicated that the susceptibility of each stone type to environmental loading, as well as the anticipated levels of residual degradation, could be qualitatively described through the parameters established by the model. This comparison not only highlights the variability in the degradation response among different stone types but also emphasizes the importance of tailored conservation strategies based on specific material properties and environmental interactions.

In particular, the experimental data collected and analyzed for Pamukkale Travertine revealed that the artificial insolation test developed for this study is likely much more aggressive than typical natural environmental loads. This finding raises important considerations for the conservation and preservation of travertine structures, as it suggests that laboratory conditions may underestimate the resilience of stone materials when subjected to real-world environmental stresses. As a result, further investigations into the long-term effects of such aggressive testing conditions on various types of stone are warranted to refine our understanding of their durability and inform better conservation practices.

Ultimately, this research underscores the critical need for ongoing studies that integrate experimental findings with predictive modelling to enhance the preservation efforts of our cultural heritage, ensuring that these invaluable artefacts can withstand the test of time.

Calculation of the actual material strength on the basis of experimentally evaluated MEI indices is an open question. Published works about relation between wave velocity and material strength present various results. The literature usually reports highly nonlinear power law relations [25,26]. An actual strength calculation (also residual one) with the addition of the phenomenological model of degradation processes presented in the paper should be based on the relevant literature, with the awareness that the relationship can be a non-linear one.

Author Contributions: Conceptualization, M.S. and A.B.; Methodology, M.S.; Data curation, M.S. and A.B.; Writing—original draft, M.S. and A.B.; Writing—review and editing, A.B.; Visualization, M.S. All authors have read and agreed to the published version of the manuscript.

Funding: This research received no external funding.

Institutional Review Board Statement: Not applicable.

Informed Consent Statement: Not applicable.

Data Availability Statement: The original contributions presented in this study are included in the [12]. Further inquiries can be directed to the corresponding author.

Conflicts of Interest: The authors declare no conflicts of interest.

References and Note

- 1. ICOMOS—ISCS. *Illustrated Glossary on Stone Deterioration Patterns*; ICOMOS International Scientific Committee for Stone (ISCS): Paris, France, 2008; Volume XV.
- 2. Irfan, T.Y.; Dearman, W.R. The engineering petrography of a weathered granite in Cornwall, England. *Q.J. Eng. Geol. Hydrogeol.* **1978**, *11*, 233–244. [CrossRef]
- 3. Bellopede, R.; Marini, P. The Effect of Water on The Strength of Building Stones. Am. J. Environ. Sci. 2012, 8, 158–161. [CrossRef]
- 4. Pinińska, J.; Domonik, A.; Dziedzic, A.; Łukasiak, D. The methodology of a complex engineering-geological approach to establish a geopark: Case study of the Malopolska Wisla River Gorge. *Geol. Q.* **2015**, *59*, 408–418. [CrossRef]
- 5. Bellopede, R.; Castelletto, E.; Marini, P. Ten years of natural ageing of calcareous stones. Eng. Geol. 2016, 211, 19–26. [CrossRef]
- 6. Barbera, G.; Barone, G.; Mazzoleni, P.; Scandurra, A. Laboratory measurement of ultrasound velocity during accelerated aging tests: Implication for the determination of limestone durability. *Constr. Build. Mater.* **2012**, *36*, 977–983. [CrossRef]

7. Heidari, M.; Torabi-Kaveh, M.; Chastre, C.; Ludovico-Marques, M.; Mohseni, H.; Hossein Akefi, H. Determination of weathering degree of the Persepolis stone under laboratory and natural conditions using fuzzy inference system. *Constr. Build. Mater.* **2017**, 145, 28–41. [CrossRef]

- 8. Martínez-Martínez, J.; Benavente, D.; Gomez-Heras, M.; Marco-Castano, L.; Ángeles García-del-Cura, M. Non-linear decay of building stones during freeze-thaw weathering processes. *Constr. Build. Mater.* **2013**, *38*, 443–454. [CrossRef]
- 9. Mutlutürk, M.; Altindag, R.; Türk, G. A decay function model for the integrity loss of stone when subjected to recurrent cycles of freezing–thawing and heating–cooling. *Int. J. Stone Mech. Min. Sci.* **2004**, *41*, 237–244. [CrossRef]
- 10. Banfill, P.F.G.; Szadurski, E.M.; Forster, A.M. Deterioration of natural hydraulic lime mortars, II: Effects of chemically accelerated leaching on physical and mechanical properties of carbonated materials. *Constr. Build. Mater.* **2016**, *111*, 182–190. [CrossRef]
- Exadaktylos, G.E.; MCDUR Partners. Elaboration of the results via sound mechanical, geometrical and physical-chemical reasons.
 Deliverable 14, Final report of the Project: Effects of the weathering on stone materials: Assessment of their mechanical durability (MCDUR), G6RD-CT2000-00266, (EC FP5, GROWTH, 2002-2005). 2005. Not published online.
- 12. Skłodowski, M.; Bobrowska, A. A generalized exponential function model of the integrity loss of stones subjected to laboratory weathering cycles. *engrXiv* **2020**. [CrossRef]
- 13. Domańska-Siuda, J.; Bagiński, B. Magma mingling textures in granitic rocks of the eastern part of the Strzegom-Sobótka Massif (Polish Sudetes). *Acta Geol. Pol.* **2019**, *69*, 143–160. [CrossRef]
- 14. Pettijohn, F.J.; Potter, P.E.; Siever, R. Sand and Sandstone; Springer: Berlin/Heidelberg Germany; New York, NY, USA, 1972.
- 15. Dunham, R.J. Classification of carbonate rocks according to depositional texture. In *Classification of Carbonate Rocks—A Symposium*; Ham, W.E., Ed.; American Association of Petroleum Geologists: Tulsa, OK, USA, 1962; Volume 1, pp. 108–121. [CrossRef]
- 16. *Standard EN* 12407:2007; Natural Stone Test Methods—Petrographic Examination. European Committee for Standarization: Brussels, Belgium, 2007.
- 17. *Standard PN-EN 12371:2010*; Methods of Testing Natural Stone—Determination of Frost Resistance. European Committee for Standarization: Brussels, Belgium, 2010.
- 18. Bobrowska, A. The Long-Term Transformation Processes of Geomechanical Properties of Macroporous Carbonate Stones in Building Construction Elements. Ph.D. Thesis, Library of Faculty of Geology, Warsaw University, Warsaw, Poland, 2014. (In Polish)
- 19. *Standard PN-EN 12370:2001*; Methods of Testing Natural Stone—Determination of Resistance to Salt Crystallization. European Committee for Standarization: Brussels, Belgium, 2001.
- Kachanov, M. Effective Elastic Properties of Cracked Solids: Critical Review of Some Basic Concepts. Appl. Mech. Rev. 1992, 45, 304–335. [CrossRef]
- 21. Wang, J.; Ahmed, B.; Huang, J.; Nong, X.; Xiao, R.; Abbasi, N.S.; Alidekyi, S.N.; Li, H. Physical and Mechanical Properties and Constitutive Model of Rock Mass Under THMC Coupling: A Comprehensive Review. *Appl. Sci.* **2025**, *15*, 2230. [CrossRef]
- 22. Ambroziak, A.; Kłosowski, P. Survey of modern trends in analysis of continuum damage mechanics. *Task Q.* **2007**, *10*, 437–454. Available online: https://journal.mostwiedzy.pl/TASKQuarterly/article/view/2095/2009 (accessed on 12 November 2025).
- 23. Pęski, Z.; Ranachowski, J. Method of and Apparatus for Generating Acoustic Surface Waves. Patent 142739, 31 March 1987. Available online: https://eprofil.pue.uprp.gov.pl/public/registry/view/Pat.142739 (accessed on 13 May 2019).
- Gawin, D.; Koniorczyk, M.; Pesavento, F. Modelling of hydro-thermo-chemo-mechanical phenomena in building materials, Bulletin of the Polish Academy of Sciences. *Tech. Sci.* 2013, 61, 51–63. [CrossRef]
- 25. Rezaei, M.; Koureh Davoodi, P. Determining the relationship between shear wave velocity and physicomechanical properties of rocks. *Int. J. Min. Geo-Eng.* **2021**, *55*, 65–72. [CrossRef]
- 26. Report on Methods for Estimating In-Place Concrete Strength American Concrete Institute. ACI 228.1R. 2003. Available online: http://civilwares.free.fr/ACI/MCP04/2281r_03.PDF (accessed on 13 November 2025).

Disclaimer/Publisher's Note: The statements, opinions and data contained in all publications are solely those of the individual author(s) and contributor(s) and not of MDPI and/or the editor(s). MDPI and/or the editor(s) disclaim responsibility for any injury to people or property resulting from any ideas, methods, instructions or products referred to in the content.